[1]M. DiDomenico, Jr., J. M. Dishman, and K. P. Sinha, Phys. Rev. B **4**, 1270 (1971).
[2]R. Z. Bachrach and O. G. Lorimor, Phys. Rev. B 6, 700 (1973).
[3]J. D. Cuthbert, C. H. Henry, and P. J. Dean, Phys. Rev. **170**, 739 (1968).
[4]T. N. Morgan, B. Welber, and R. N. Bhargava, Phys. Rev. **166**, 751 (1968).
[5]R. Z. Bachrach, Rev. Sci. Instrum. **43**, 734 (1972).
[6]J. M. Dishman, M. DiDomenico, Jr., and R. Caruso, Phys. Rev. B **2**, 1988 (1970).
[7]J. S. Jayson and R. W. Dixon, J. Appl. Phys. **42**, 774 (1971). This paper also utilizes impulse measurements to evaluate minority-carrier lifetimes. We note here, by way of clarification, that the impulse techniques measure the "fast" minority-carrier lifetime, i.e., the parallel capture rates of all centers, and does not measure the effect of rethermalization of these trapped minority carriers.
[8]J. S. Jayson and R. Z. Bachrach, Phys. Rev. B **4**, 477 (1971).
[9]J. S. Jayson, R. Z. Bachrach, P. D. Dapkus, and N. E. Schumaker, Phys. Rev. B 6, 2357 (1972).
[10]J. S. Jayson, R. N. Bhargava, and R. W. Dixon, J. Appl. Phys. **41**, 4972 (1970).
[11]K. P. Sinha and M. DiDomenico, Jr., Phys. Rev. B **1**, 2623 (1970).
[12]G. E. Neumark, Phys. Rev. B **5**, 408 (1972).
[13]G. W. Castellan and F. Seitz, *Semiconducting Materials* (Butterworths, London, 1951).
[14]K. Colbow, Phys. Rev. **141**, 742 (1966).
[15]J. M. Dishman, Phys. Rev. B **3**, 2588 (1971).
[16]R. N. Bhargava, Phys. Rev. B **2**, 387 (1970).
[17]C. H. Henry, P. J. Dean, and J. D. Cuthbert, Phys. Rev. 166, 754 (1968).
[18]F. J. Blatt, *Physics of Electronic Conduction in Solids* (McGraw-Hill, New York, 1968), p. 179.
[19]D. R. Hamann and A. L. McWhorter, Phys. Rev. 134, A250 (1964).
[20]E. F. Smith and P. T. Landsberg, J. Phys. Chem. Solids **27**, 1727 (1966).
[21]C. H. Henry, S. E. Schnatterly, and C. P. Slichter, Phys. Rev. 137, A583 (1965).
[22]D. L. Dexter, Solid State Phys. **6**, 353 (1958).
[23]H. C. Casey, Jr., F. Ermanis, and K. B. Wolfstirn, J. Appl. Phys. **40**, 2945 (1969).
[24]J. G. Gay, Phys. Rev. B **4**, 2567 (1971).
[25]J. M. Dishman, Phys. Rev. B 6, 1337 (1972).
[26]J. M. Dishman and I. Camlibel, Phys. Rev. B 6, 1340 (1972).
[27]J. D. Cuthbert and D. G. Thomas, Phys. Rev. **154**, 763 (1967).
[28]J. M. Dishman, Phys. Rev. B **5**, 2258 (1972).

PHYSICAL REVIEW B VOLUME 7, NUMBER 6 15 MARCH 1973

Second-Order Raman Spectrum of Germanium

B. A. Weinstein* and Manuel Cardona
Max-Planck-Institut für Festkörperforschung Stuttgart, Bundesrepublik Deutschland
(Received 5 October 1972)

The second-order Raman spectrum of crystalline germanium has been observed. Measurements were performed for several incident- and scattered-light polarizations so as to separate the three independent components of the Raman tensor. Interpreted in the light of recent neutron-scattering work by Nelin and Nilsson, the Γ_1 spectrum corresponds to overtone two-phonon processes. Overtone and combination processes are seen for the $\Gamma_{25'}$ and Γ_{12} components.

I. INTRODUCTION

Two-phonon processes in the Raman spectrum of silicon were first reported by Parker *et al.*[1] More recent measurements[2,3] used several sample orientations and polarization configurations so as to obtain the three independent components of the Raman tensor. It was shown that the Γ_1 component of the Raman tensor, much stronger than the Γ_{12} and $\Gamma_{25'}$ counterparts, is due almost exclusively to two-phonon overtones. A rather close correspondence between the Γ_1 component and the density of two-phonon overtone states, obtained from the density of one-phonon states, was established. Similar measurements for GaP reveal two-phonon combination processes for the Γ_{15} Raman spectrum.[2]

The second-order Raman spectra are very weak in comparison with the allowed first-order line ($\Gamma_{25'}$ symmetry). They can nevertheless be easily observed in GaP and Si because, in these materials, only weak indirect transitions take place at the wavelengths of the conventional lasers used in Raman work (He-Ne, A ion, Kr ion). The penetration depth of the laser is quite considerable ($\sim 10^{-3}$ cm) and the amount of scattered light correspondingly large. In germanium, however, this penetration depth is less than 10^{-4} cm and the second-order scattering becomes very weak. While considerable work has been done on the first-order scattering of this material,[1,4-6] the two-phonon second-order spectrum has not been previously reported.

In this work we present data for the three irreducible components of the second-order Raman spectrum of germanium at room temperature. The results, while similar to those previously reported for silicon,[2,3] offer some new features towards the high-frequency end, probably related to the fact that an electronic resonance (E_1, $E_1+\Delta_1$) occurs

near the laser frequency used. The observed spectra can be interpreted rather accurately due to the existence of very precise neutron data for the phonon spectrum of this material and the corresponding density of states.[7,8]

II. EXPERIMENT

The Ge sample was a single crystal nearly intrinsic at room temperature ($\rho \approx 30\ \Omega$cm, n type). It was oriented to $\pm 1^\circ$ using x rays mechanically polished and etched by performing a final polishing with Syton.[9] With this procedure a surface is obtained which is smoother than that prepared with conventional chemical etching.

Measurements were made for four different scattering geometries, shown in Table I. The backscattering configuration was used throughout, with a (100) sample surface. Although the angle of incidence was 30°, the incident and the scattered wave vectors are nearly perpendicular to the sample surface because of the large refractive index of the material. To minimize residual errors due to the finite angle of incidence, the incident polarization was always chosen in the plane of the sample. Since in a cubic material the symmetric Raman tensor has only three independent components (the irreducible components Γ_1, Γ_{12}, $\Gamma_{25'}$ of a second-rank tensor),[10,11] three independent measurements suffice to separate them; the fourth measurement of Table I can be used as a check.[2] The combination of irreducible components measured for each of our experimental configurations is also shown in Table I.

The measurements were performed with the 5145-Å line of an argon-ion laser at a power of 1.5 W. In order to reduce the level of scattered light, which is quite high for such strong laser power, a Spex triple-monochromator system was used. The sample area was purged with He gas so as to eliminate the strong scattering from air in the region 50–150 cm^{-1}. The signal was detected by photon counting and the counts stored as a function of wave number in the 1024 channels of a multichannel analyzer. The spectrometer slits were set for a resolution of 4 cm^{-1}. The sample was kept at room temperature during the measurements The laser beam was focused on the sample with a cylindrical lens in order to spread it out and avoid local heating. Even so, a slight shift was observed in the first-order line with respect to its room-temperature position. From the temperature dependence of this line reported by Cerdeira and Cardona[4] we infer that the effective sample temperature was about 330 °K.

TABLE I. Scattering configurations used in our experiments. The crystal surface was a (100) plane. $\hat{e}_i$ and $\hat{e}_s$ are the polarizations of the incident and scattered photons.

Measurement	Geometry	Symmetry component
1	$\hat{e}_i \parallel [010]$ $\hat{e}_s \parallel [010]$	$\Gamma_1 + 4\Gamma_{12}$
2	$\hat{e}_i \parallel [010]$ $\hat{e}_s \parallel [001]$	$\Gamma_{25'}$
3	$\hat{e}_i \parallel [01\bar{1}]$ $\hat{e}_s \parallel [011]$	$3\Gamma_{12}$
4	$\hat{e}_i \parallel [01\bar{1}]$ $\hat{e}_s \parallel [01\bar{1}]$	$\Gamma_1 + \Gamma_{12} + \Gamma_{25'}$

III. RESULTS AND DISCUSSION

Figure 1 displays the experimental Raman spectra of Ge between 50 and 650 cm^{-1} found for configurations 1, 2, and 3 of Table I. The first-order line (off scale) peaks at 299.7 cm^{-1} (330 °K). Since the memory of the multichannel analyzer could not accomodate the entire wave-number range, each spectrum shown in Fig. 1 was taken in two separate runs. The curves of Fig. 1 display the essential reproducible features of the spectra. The arrows in the figure show the position of critical points in the density of two-phonon states, as determined from Nelin and Nilsson's neutron-scattering measurements.[8] The numbers in parentheses after each critical point refer to the corresponding branch of the phonon dispersion curves, labeled in order of increasing energy. Only critical points in the density of overtone two-phonon states are given, since most of the structure can be explained as due to phonon overtones.[2,3] Also, while the density of two-phonon overtones can be immediately obtained from the one-phonon density given in Ref. 8 by doubling the frequency scale, the density of two-phonon combination requires an appropriate integration of the phonon dispersion curves which we have not performed. Since Nelin and Nilsson's measurements were taken at 80 °K, we have made a minor correction in the position of the critical points. They were shifted downward in energy by an amount proportional to their energy, so as to have the first-order Raman line at 299.7 cm^{-1}, as measured in our experiment at 330 °K.

Figure 2 contains a plot of the experimental overtone density of two-phonon states, from the work of Nelin and Nilsson, superimposed on our Raman spectrum of symmetry composition $\Gamma_1 + 4\Gamma_{12}$. This spectrum, however, has been divided by $(n_B+1)^2$, where n_B is the Bose–Einstein occupation factor. The density of states is the single phonon density with the frequency scale doubled and the temperature correction mentioned above. The arrows indicate two-phonon overtone critical points. We emphasize that this density of states is essentially

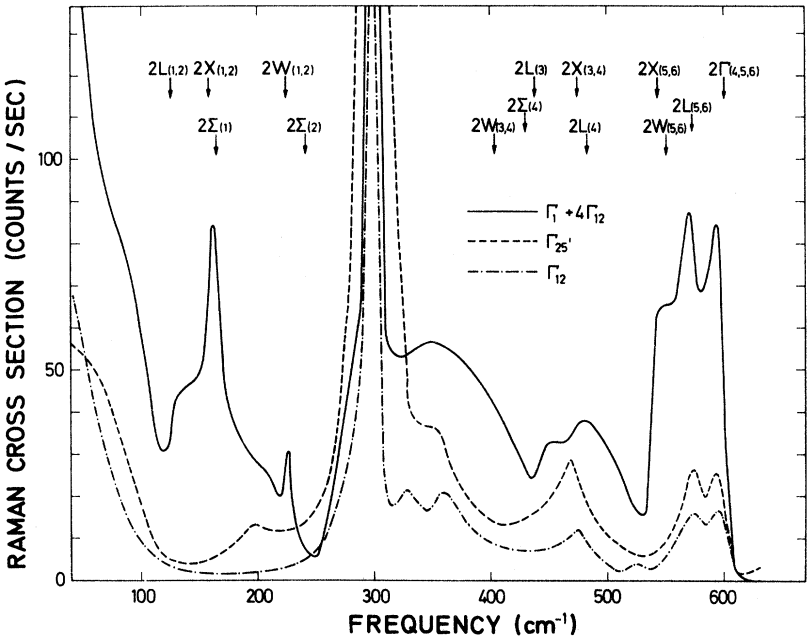

FIG. 1. Raman spectra obtained for germanium in the configurations 1–3 of Table I at room temperature. The allowed first-order line of $\Gamma_{25'}$ symmetry reaches the strength 6000 counts/sec, and the forbidden ones, of symmetry $\Gamma_1+4\Gamma_{12}$ and $3\Gamma_{12}$, respectively, reach 500 and 240 counts/sec. The energies of two-phonon overtone critical points are indicated by arrows.

experimental. Over 500 phonon frequencies uniformly distributed throughout an irreducible section of the Brillouin zone were measured with an accuracy better than 1%. Even so, interpolation was necessary in order to obtain the density of states. It was accomplished with a Born–von Kármán model fitted to the experimental data along the Δ, Λ, Σ symmetry directions (see Fig. 3) and slightly corrected so as to fit the measured points surrounding each interpolated point.[8]

The overtone density of states is especially useful in analyzing the Γ_1 component of the Raman spectrum. Overtone two-phonon states must always contain this representation. Similarly, combination two-phonon states *belonging to different irreducible representations* never contain Γ_1. Furthermore, it has been experimentally verified[2,3] in Si and GaP that the Γ_1 component of the Raman spectrum of these materials contains mostly two-phonon overtones.

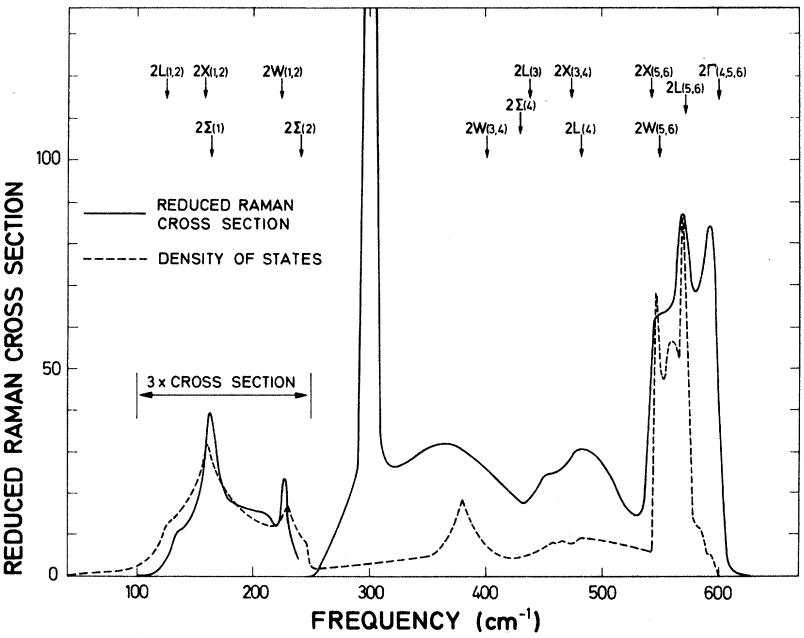

FIG. 2. Reduced [experimental spectrum divided by $(n_B+1)^2$] $\Gamma_1+4\Gamma_{12}$ component of the Raman spectrum of germanium compared with the density of two-phonon overtone states.

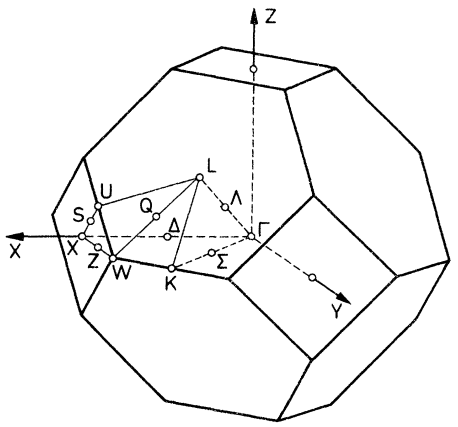

FIG. 3. Brillouin zone of germanium indicating the most important symmetry points and lines.

Since the Γ_{12} component of the Raman spectrum is very small and contains little structure, we may treat the $\Gamma_1 + 4\ \Gamma_{12}$ spectrum as consisting solely of Γ_1. In the regions where this is not strictly true it is obvious what would be the result of subtracting the Γ_{12} component. In Fig. 2 we see that the Γ_1 Raman structure between 120 and 250 cm^{-1} is due to two-phonon overtone states of the two lowest [transverse acoustical (TA)] branches. The structure emerges from the steep low-energy line at 120 cm^{-1} (see Fig. 1). It peaks at 163 cm^{-1} with an M_1 singularity due to phonons at X in the degenerate branches 1 and 2 and an M_2 singularity from Σ in branch 1. The maximum occurring at 228 cm^{-1} is due to an M_1 singularity at W and an M_2 singularity with coordinates (0.9, 0.5, 0.1) on the surface of the Brillouin zone (Q point, Fig. 3), both in branch 2. The structure ends at 250 cm^{-1} with an M_3 critical point in branch 2 at another low-symmetry point on the surface of the Brillouin zone. This point has coordinates (0.69, 0.69, 0.12) and lies on the line L-K (see Fig. 3). The critical point at Σ in branch 2 is of type M_2 and therefore cannot be associated with the end of the TA spectrum of Fig. 2.

The forbidden first-order peaks of configurations 1 and 3 (Table I) are higher than the corresponding second-order spectra. This is in contrast to the case of Si,[3] where the forbidden first-order lines are weaker than the prominent second-order acoustical and optical structure. The question then arises as to whether the forbidden lines are intrinsically induced by some mechanism, such as spatial dispersion[12] or surface electric fields,[13] or are simply a result of slight misorientations and/or poor surface conditions. Recent measurements[14] of resonant Raman scattering of this forbidden line around the E_1 gap give the same shape as that of the allowed line. A sharper resonance is expected for truly forbidden lines,[15] and thus we believe that the present forbidden lines are primarily a result of misorientation and surface conditions.

The broad peak in the Raman spectrum of Fig. 2 just above the first-order line can be associated with the density-of-states peak at 380 cm^{-1}. The breadth of this Raman peak may be due to some contributions from TA + TO combinations. The Raman structure between 430 and 530 cm^{-1} is due to the similarly shaped density-of-states structure in that region.

The strong scattering in the region 535–610 cm^{-1} is due to the optical phonons. We have studied this region in detail and display the results in Figs. 4 and 5. In Fig. 4 we have decomposed the Raman spectrum into its individual symmetry components Γ_1, $\Gamma_{25'}$, and Γ_{12}. As in the case of Si, the Γ_1 component is dominant and Γ_{12} is small.[2,3] In Fig. 5 we have summed the three spectra, computing $\Gamma_1 + \Gamma_{25'} + \Gamma_{12}$ at several frequencies, and plotted the result with the corresponding error bars along with the experimentally measured spectrum of composition $\Gamma_1 + \Gamma_{25'} + \Gamma_{12}$ (measurement 4 of Table I). Good agreement is obtained.

In Fig. 4 we have again indicated the overtone critical points as determined from Ref. 8. The structure begins close to the M_0 singularity at X in the branches 5 and 6 (at 542.5 cm^{-1}). In the density of states (see Fig. 2) there is a peak at 546 cm^{-1} due to the M_1 and M_2 singularities at the points Q and S, respectively, in branch 5. S is another low-symmetry point on the surface of the Brillouin zone with coordinates (0.85, 0.45, 0.0) (X-U line of Fig. 3). This peak corresponds to the weak peak, more nearly a shoulder, in the Raman spectrum at 546 cm^{-1}. Further, the density of states shows a minimum due to an M_3 critical point at W in branch 5 at 549 cm^{-1} and a small maximum at 560 cm^{-1} (see Fig. 2). These features do not appear resolved in the Raman spectrum. They seem to be broadened into the shoulder just mentioned. The next peak in the Raman spectrum occurs at 572 cm^{-1}. It coincides with the M_2 critical point in the sixth branch at L.

The density of states now falls rapidly to zero at twice the first-order $\vec{k} \neq 0$ Γ-point Raman frequency. However, the second-order Raman spectrum has another large peak at 594 cm^{-1} and does not go to zero until 610 cm^{-1}, well beyond the expected zero of 599.4 cm^{-1} (sample at 330 °K). This situation is in contrast to Si, where the termination of the second-order Raman spectrum occurs at exactly twice the first-order frequency.[2,3]

The anomalous peak at 594 cm^{-1} occurs only six wave numbers below the frequency of the two-Γ-phonon overtone. Thus it is probably related to the creation of two phonons of opposite wave vector near but not exactly at Γ. The fact that these phonons scatter much more than their density of states

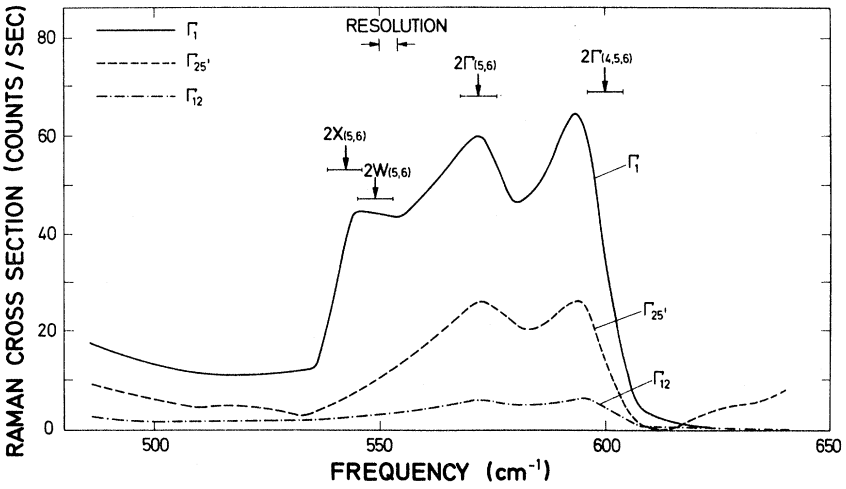

FIG. 4. Irreducible components of the Raman tensor observed for germanium in the region of two-TO-phonon overtones.

suggests (see Fig. 2) can be related to the fact that the laser line used falls near the E_1 resonant gap.[5] A similar effect has been observed for GaP: A 2Γ peak appears near the E_0 resonance, but away from it results in agreement with the density of states are obtained.[16,17] The failure to observe the anomalous 2Γ peak for Si would then be due to the fact that only measurements away from the resonance have been performed.[2,3] It would therefore be of interest to measure the two-phonon spectrum for several laser wavelengths. Unfortunately, the large powers required by the small scattering cross sections only enable us to use the 5145- and 4880-Å lines of the A-ion laser. Preliminary measurements with the 4880-Å line do indeed suggest some change in the ratio of the strength of the 572- and 594-cm^{-1} peaks of Fig. 4. The origin of the strong resonance of the two-phonon pairs near Γ will be discussed elsewhere.[16]

We should at this point mention that Solin and Ramdas[18] have observed a peak in the second-order Raman spectrum of diamond at a frequency slightly

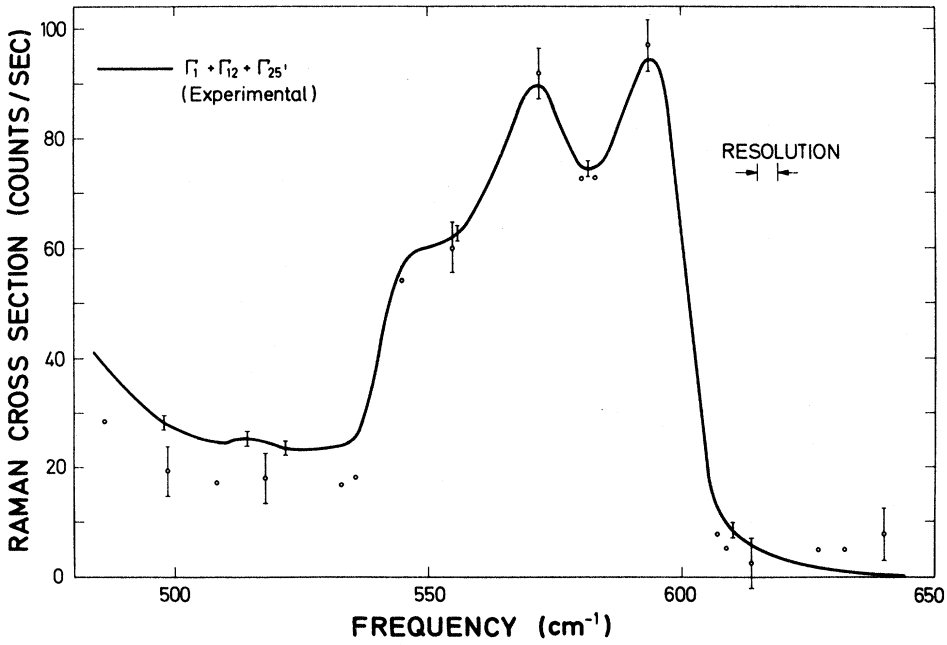

FIG. 5. Experimentally found $\Gamma_1+\Gamma_{12}+\Gamma_{25'}$ component of the Raman tensor (solid line) compared with the points with error flags obtained as linear combinations of the measurements of Fig. 4.

above twice that of the $\vec{k}=0$ phonon ($2\omega_R$). They suggest the shift may be due to anharmonic interactions. More recent infrared measurements, however, give a two-phonon peak slightly *below* $2\omega_R$.[19] In view of the uncertain experimental situation and of the considerable current theoretical activity on two-phonon anharmonic shifts, we abstain from further comments on this matter.

The acoustical portion of the reduced Raman spectrum of Fig. 2 (100–250 cm^{-1}) has been multiplied by 3 in order to better show its detail. It is clear then that the reduced Raman spectrum in this region is much weaker than what is suggested by the density of states. This fact is even more striking if one bears in mind that the factor which enters into the scattering amplitude[10] has not been taken out of the experimental curve. We thus conclude that the coupling constant for the acoustical phonons is much smaller than for the optical ones. Similar effects have been observed in the first-order Raman spectrum of amorphous Ge.[20]

The $\Gamma_{25'}$ spectrum of Fig. 1 has two major features other than the first-order line. The only possible overtone candidates for the peak at 468 cm^{-1} in the $\Gamma_{25'}$ spectrum are the X and L critical points of branch 4 (see Fig. 1). They occur, however, a little high in frequency and their strength would be too small to account for the observations unless an unusually high matrix element were associated with this process. The observed structure is also much sharper than the density of overtone states just discussed (see Fig. 2). We therefore prefer to assign this structure in the $\Gamma_{25'}$ component of the Raman spectrum (also in the Γ_{12}) around 468 cm^{-1} to two-phonon combination processes. Combination processes are also largely responsible for the components of the Raman spectrum of GaP other than Γ_1.[2] We note that the Raman peak at 468 cm^{-1} is similar in form to the structure in the density of overtone states which peaks at 380 cm^{-1}. The phonons in this peak are thus prime candidates for one of the phonons of the combination state. The peak at 380 cm^{-1} is due to M_1- and M_2-type singularities, respectively, at the low-symmetry point Q and a point on the line L-K (see Fig. 3). Conservation of $\vec{k}$ requires the other contributor to the combination state to have equal and opposite wave vector. In order that the two-phonon combination state should have the proper energy we must look for overtone structure in the region 556 cm^{-1}. Then the average of 556 and 380 cm^{-1} gives 468 cm^{-1}, the frequency of the Raman structure of interest. At 556 cm^{-1} one finds a rather flat region of the second-order Raman spectrum between the critical points W and L. It can be seen in Fig. 3 that there is also in this region a Q critical point (W-L line). We can therefore construct two-phonon states of zero $\vec{k}$ vector by combining the phonons around 380/2 cm^{-1} with those around 556/2 cm^{-1}. While a calculation of the corresponding combined density of states has not been performed, it is easy to conjecture that the combination of the triangular shape of the 380-cm^{-1} peak with the sharp rectangular one of the 556-cm^{-1} structure should give a triangular peak of the type observed for the $\Gamma_{25'}$ component of Fig. 1. The $\Gamma_{25'}$ structure between 535 and 610 cm^{-1} (Fig. 4) is probablv due to overtone states analogous to the corresponding Γ_1 structure. A similar result was also found for Si.[2,3] The structure begins with an M_0 singularity at X from branches 5 and 6 at 542.5 cm^{-1}. It then rises to a peak at 572 cm^{-1}, corresponding to the M_2 singularity in branch 6 at L. Here we expect a strong $\Gamma_{25'}$ contribution from the L point because the phonons involved have L_3 symmetry and the product $L_3 \otimes L_3$ when reduced contributes twice to $\Gamma_{25'}$ but only once to Γ_1 and Γ_{12}. The Raman structure "ignores" the singularities at Q, S, and W between X and L, rising smoothly in this region. Finally, the $\Gamma_{25'}$ structure, for reasons not yet known, also shows a peak at 594 cm^{-1} and does not go to zero until about 610 cm^{-1}.

The Γ_{12} scattering is found to be weak and almost structureless, as was the case in Si and GaP.[2,3] An explanation of this weakness and the predominance of Γ_1 is still awaited. Cowley has performed a calculation of the second-order Raman scattering of Si and Ge with a model polarizability represented by one adjustable parameter.[21] The results are crude and do not explain the experimental observations.[2,3] However, the model does predict a very small contribution of the acoustical phonons relative to the optical ones. Bruce and Cowley[22] have had some success in calculating the Γ_1, $\Gamma_{25'}$, and Γ_{12} Raman spectra of KBr using a breathing-shell model. However, the model contains three adjustable parameters which are difficult to relate to microscopic properties.

The small peak in the Γ_{12} spectrum near 470 cm^{-1} is again assumed to be associated with combination states, as for $\Gamma_{25'}$. The Γ_{12} structure from 535 to 610 cm^{-1} can be discussed in the same manner as the corresponding Γ_1 and $\Gamma_{25'}$ structures.

IV. SUMMARY

We have shown that the second-order Raman-scattering spectrum of Ge can be well understood in terms of the experimental density of phonon states measured by Nelin and Nilsson. The Γ_1 component of the scattering is almost completely due to overtone states and mirrors the experimental density of two-phonon overtone states. Important exceptions occur in the optical region. Here we find a shoulder where two peaks occur in the density of states and an additional anomalous peak

occurs at a point where the density of two-phonon states vanishes. The existence of this anomalous structure may be a resonance effect which emphasizes scattering by two phonons near Γ. The $\Gamma_{25'}$ spectrum can be understood in terms of two-phonon overtone and combination states, while the Γ_{12} spectrum is seen to be relatively unimportant.

ACKNOWLEDGMENTS

We would like to thank Dr. R. Reed for suggesting the He purging of the sample, Professor H. Bilz for discussions concerning the $\Gamma_{15'}$ Raman components, and Professor C. E. Hathaway for a preprint of his work.

*On leave from Brown University, Providence, R. I. 02912.

[1]J. H. Parker, Jr., D. W. Feklman, and M. Askin, Phys. Rev. 155, 712 (1967).

[2]B. A. Weinstein and Manuel Cardona, Solid State Commun. 10, 961 (1972).

[3]Paul A. Temple and C. E. Hathaway, Phys. Rev. B (to be published).

[4]Fernando Cerdeira and Manuel Cardona, Phys. Rev. B 5, 1440 (1972).

[5]F. Cerdeira, W. Dreybrodt, and Manuel Cardona, Solid State Commun. 10, 591 (1972).

[6]R. K. Ray, R. L. Aggarwal, and B. Lax, in *Light Scattering in Solids*, edited by M. Balkanski (Flammarion, Paris, 1971), p. 288.

[7]G. Nilsson and G. Nelin, Phys. Rev. B 3, 364 (1971).

[8]G. Nelin and G. Nilsson, Phys. Rev. B 5, 3151 (1972).

[9]Syton HT-50 colloidal solution, Monsanto Chemical Co., St. Louis, Mo. We are thankful to Dr. D. E. Aspnes for suggesting to us the use of this polishing etchant.

[10]R. A. Loudon, Adv. Phys. 13, 423 (1964).

[11]We have found no evidence for the antisymmetric tensor component $\Gamma_{15'}$. This component may become important for laser lines closer to the resonant E_1 or $E_1+\Delta_1$ gaps.

[12]R. Martin and T. C. Damen, Phys. Rev. Lett. 26, 86 (1971).

[13]P. Corden, A. Pinczuk, and E. Burstein, in *Proceedings of the Tenth International Conference on the Physics of Semiconductors, Cambridge*, 1970, edited by S. P. Keller, J. C. Hensel, and F. Stern (U. S. AEC, Oak Ridge, Tenn., 1970), p. 739.

[14]J. Renucci and F. Cerdeira (private communication).

[15]F. Cerdeira, W. Dreybrodt, and Manuel Cardona, in *Proceedings of the Eleventh International Conference on the Physics of Semiconductors, Warsaw* (Polish Scientific Publishers, Warsaw, 1972), p. 1142.

[16]B. Weinstein and M. Cardona (unpublished).

[17]J. F. Scott, T. C. Damen, R. C. C. Leite, and W. T. Silfvast, Solid State Commun. 7, 953 (1969).

[18]S. A. Solin and A. K. Ramdas, Phys. Rev. B 1, 1687 (1970).

[19]J. F. Angress and A. J. Maiden, J. Phys. C 4, 235 (1971).

[20]J. E. Smith Jr., M. H. Brodsky, B. L. Crowder, M. I. Nathan, and A. Pinczuk, Phys. Rev. Lett. 26, 642 (1971).

[21]R. A. Cowley, J. Phys. (Paris) 26, 659 (1965).

[22]A. D. Bruce and R. A. Cowley, J. Phys. C. 5, 595 (1972).

PHYSICAL REVIEW B VOLUME 7, NUMBER 6 15 MARCH 1973

Impact Ionization, Breakdown, and Photoinduced Switching in CdSe

R. P. Khosla, J. R. Fischer, and B. C. Burkey

Research Laboratories, Eastman Kodak Company, Rochester, New York 14650

(Received 11 September 1972)

Measurements of conductivity, Hall coefficient, and mobility of CdSe single crystals have been made in the temperature range 4.2–300 °K. For the sample with the lowest carrier concentration of 2.8×10^{15} cm^{-3}, the donor ionization energy of 18 meV is obtained. This is in good agreement with the calculated hydrogenic value of 19 meV. Above 100 °K, the electron–polar-optical-phonon interaction determines the mobility. Below 100 °K, ionized- and neutral-impurity scattering also contribute to the mobility, and for $T < 50$ °K dominate the mobility. At relatively low fields, nonlinear I-V characteristics are observed. The samples show breakdown around 100 V/cm (varies somewhat with carrier concentration), resulting in a region of current-controlled negative resistance. The conductivity, Hall coefficient, and mobility of the samples are measured in the high-field region. The samples which show current-controlled negative resistance can be switched from a low- to a high-conductivity state under illumination below the threshold field in the dark. The higher the intensity of illumination, the lower is the threshold field for switching. These results are discussed in terms of various models.

I. INTRODUCTION

Impact ionization of shallow donor and acceptor states has been observed in several semiconductors, namely, Ge,[1–3] GaAs,[4,5] and CdS.[6] Experimentally, a rapid increase in current is observed at a threshold electric field. In those cases for which the Hall coefficient can also be measured,